Characterization of symmetric [3 x 3] directional couplers fabricated by direct writing with a femtosecond laser oscillator

Kenya Suzuki, Vikas Sharma, James G. Fujimoto, Erich P. Ippen

Department of Electrical Engineering and Computer Science and Research Laboratory of Electronics, Massachusetts Institute of Technology Cambridge, MA 02139
kenya@aecl.ntt.co.jp, vsharma@mit.edu, jgfuji@mit.edu, ippen@mit.edu

Yusuke Nasu

NTT Photonics Laboratories, NTT Corporation, 3-1 Morinosato Wakamiya, Atsugi, Kanagawa, 243-0198, Japan
nasu@aecl.ntt.co.jp

Abstract: We demonstrate and characterize symmetric [3x3] three-dimensional directional couplers fabricated in glass using a high-pulse energy femtosecond laser oscillator. The characteristics of the [3x3] directional couplers closely agree with the theoretical prediction, except for small errors caused by the fabrication process. We show that deviations from symmetry are dominated by vertical position errors of the coupling waveguide.

OCIS codes: (140.3390) Laser materials processing; (190.4180) Multiphoton processes; (230.7370) Waveguides; (320.7110) Ultrafast nonlinear optics.

References and links

1. S. K. Sheem, "Optical fiber interferometers with [3x3] directional couplers: Analysis," J. Appl. Phys. **52**, 3865-3872 (1981).
2. K. Takada, H. Yamada, and M. Horiguchi, "Optical low coherence reflectometer using [3x3] fiber coupler," IEEE Photonics Technol. Lett. **6**, 1014-1016 (1994).
3. M. A. Choma, C. Yang, and J. A. Izatt, "Instantaneous quadrature low-coherence interferometry with 3 x 3 fiber-optic couplers," Opt. Lett. **28**, 2162-2164 (2003).
4. K. M. Davis, K. Miura, N. Sugimoto, and K. Hirao, "Writing waveguides in glass with a femtosecond laser," Opt Lett. **21**, 1729-1731 (1996).
5. S. Nolte, M. Will, J. Burghoff, and A. Tuennermann, "Femtosecond waveguide writing; a new avenue to three-dimensional integrated optics," Appl. Phys. A **77**, 109-111 (2003).
6. Y. Nasu, M. Kohtoku, Y. Hibino, and Y. Inoue, "Three-dimensional waveguide interconnection formed with femtosecond laser in planar lightwave circuits," in *Proceedings of Optical Fiber Communication Conference, 2005. Technical Digest. OFC/NFOEC*, **4**, (Anaheim, Calif., 2005), pp. 503-505.
7. W. Watanabe, T. Asano, K. Yamada, K. Itoh, and J. Nishii, "Wavelength division with three-dimensional couplers fabricated by filamentation of femtosecond laser pulses," Opt. Lett. **28**, 2491-2493 (2003).
8. M. Kowalevicz, V. Sharma, E. P. Ippen and J. G. Fujimoto, "3D photonic devices fabricated in glass using a femtosecond laser oscillator," Opt. Lett. **21**, 1060-1062 (2005).
9. M. Kowalevicz, Jr., A. Tucay Zare, F. X. Kärtner, and J. G. Fujimoto, "Generation of 150-nJ pulses from a multiple-pass cavity Kerr-lens mode-locked Ti:Al_2O_3 oscillator," Opt. Lett. **28**, 1597-1599 (2003).
10. Kenya Suzuki NTT Photonics Laboratories, NTT Corporation, 3-1 Morinosato Wakamiya, Atsugi, Kanagawa 243-0198, Japan, Yusuke Nasu, Vikas Sharma, Takahiro Ikeda, James G. Fujimoto, Erich P. Ippen, and Michael S. Feld are preparing a manuscript to be called "Characteristics of waveguide in soda-lime glass caused by irradiation of femtosecond laser pulses."
11. R. Osellame, N. Chiodo, V. Maselli, A. Yin, M. Zavelani-Rossi, G. Cerullo, P. Laporta, L. Aiello, S. De Nicola, P. Ferraro, A. Finizio, and G. Pierattini, "Optical property of waveguides written by a 26 MHz stretched cavity Ti:sapphire Femtosecond oscillator," Opt. Express **13**, 612-620 (2005).
12. K. Okamoto, *Fundamentals of optical waveguides*, (Academic Press, 2000).
13. K. Minoshima, A. M. Kowalevicz, E. P. Ippen, and J. G. Fujimoto, "Fabrication of coupled mode photonic devices in glass by nonlinear femtosecond laser materials processing," Opt. Express **10**, 645-652 (2002).

#10011 - $15.00 USD Received 16 December 2005; revised 3 March 2006; accepted 5 March 2006

1. Introduction

Optical, symmetric [3x3] directional couplers [1] are useful for optical interferometer-based sensors because they enable the detection of the direction of an interferometer arm phase change caused by an analyte. A Michelson interferometer-based low-coherence reflectometer and optical coherence tomography have already been demonstrated by using a symmetric [3x3] directional coupler for optical signal processing [2, 3]. Although these sensors employ fiberoptic [3x3] couplers, an integrated optic form for these devices is preferable because it offers such advantages as flexibility in photonic circuit configuration and mass production. Even in an integrated optic form, it is important to maintain the symmetry of the waveguide arrangement in the coupling region in order to be able to detect the direction of phase change efficiently in Mach-Zehnder interferometer-based sensors. However, conventional waveguide fabrication techniques based on planar technology that utilize photolithography and dry etching techniques are unsuitable for realizing three-dimensional devices such as symmetric [3x3] directional couplers.

Waveguide fabrication techniques that use femtosecond laser pulses to write waveguides in solid glass are a promising approach for the above purpose. Photosensitivity phenomena in transparent glass materials were first observed and demonstrated by Davis in 1996 [4]. This material-processing technique utilizes nonlinear or multiphoton absorption of a focused, high-intensity laser beam. Many photonic devices have already been demonstrated that take advantage of three-dimensional structural fabrication, including optical splitters [5], interconnections [6], and WDM couplers [7]. We previously reported a [3x3] directional coupler for the wavelength range of 800 nm [8]. In this paper, we provide a detailed characterization and description of a symmetrical [3x3] directional coupler for the wavelength range of 1500 nm and investigate both the origin of fabrication errors and how they change device characteristics.

2. [3x3] directional coupler

Figure 1 shows the schematic configuration of a symmetric [3x3] directional coupler and its typical coupling characteristics. The coupler consists of three input waveguides, a transition region, a coupling region, a second transition region, and output waveguides. The mode coupling equations for [3x3] directional couplers are described in reference [1]. Here we summarize this formalism and expand it by including the mismatches in the propagation constants between the waveguides in the coupling region, so that we can later analyze the coupler characteristics in detail. The general mode coupling equations of a [3x3] coupler are represented as:

$$\begin{aligned}
&\frac{dA_1}{dz} + j\kappa_{12}A_2 e^{-j2\delta_{21}z} + j\kappa_{13}A_3 e^{+j2\delta_{13}z} = 0 \\
&\frac{dA_2}{dz} + j\kappa_{23}A_3 e^{-j2\delta_{23}z} + j\kappa_{21}A_1 e^{+j2\delta_{21}z} = 0 \\
&\frac{dA_3}{dz} + j\kappa_{31}A_1 e^{-j2\delta_{13}z} + j\kappa_{32}A_2 e^{+j2\delta_{23}z} = 0
\end{aligned} \tag{1}$$

where, Ai, κ_{ij}, and δ_{ij} are the electromagnetic fields of waveguide i, and the coupling coefficients and propagation constant differences between coupling waveguides i and j, respectively. Derivations are described in more detail in the appendix. In an ideal case, where we can ignore asymmetry in the equations, the parameters satisfy the conditions $\delta_{ij} = 0$, $\kappa_{ij} = \kappa$. Figure 1(b) shows the calculated coupling characteristics of an ideal symmetric [3x3] directional coupler, where an optical signal is launched into input port waveguide 1. It should be noted that the optical power of waveguide 1 gradually couples with waveguides 2 and 3 at the same ratio, but it never falls to zero. This is because part of the input optical signal, which

#10011 - $15.00 USD Received 16 December 2005; revised 3 March 2006; accepted 5 March 2006

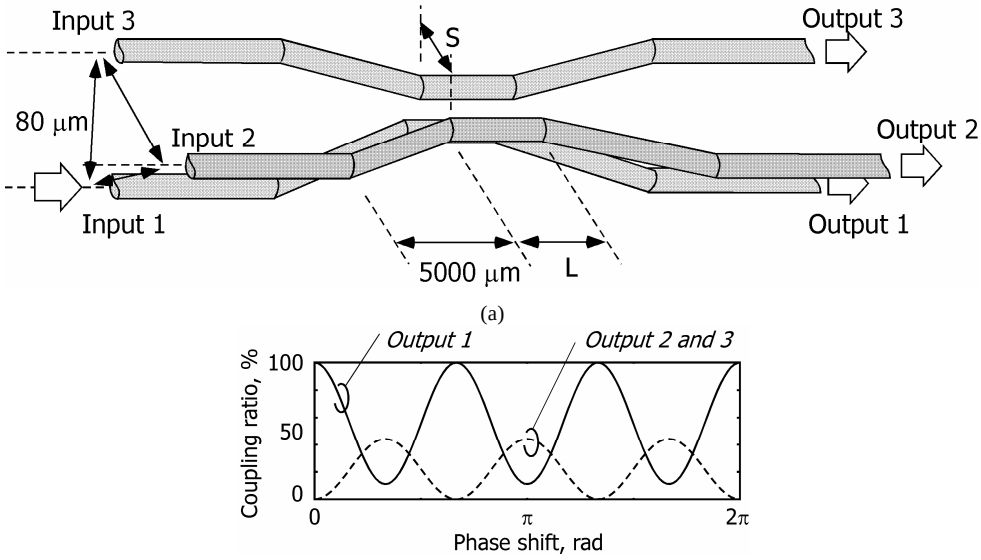

Fig. 1. (a) Schematic configuration of a [3x3] directional coupler, and (b) characteristics of an optical, symmetric [3x3] directional coupler.

couples with waveguide 2, is transferred back to waveguides 3 and 1. The same is true of the part of the input signal that couples with waveguide 3, and is transferred back to waveguides 2 and 1. In other words, if we launch an optical signal from input port 1 and monitor output 1, then the coupler becomes an asymmetric directional coupler. Therefore, output 1 does not fall to zero.

3. Experiment

We fabricated the symmetric [3x3] directional couplers by using a high-pulse energy, KLM Ti:Al_2O_3 oscillator with a multi pass cavity. This laser design has been described in detail in previous publications. The repetition rate and pulse duration of the oscillator were 5.85 MHz and 67 fs, respectively [9]. The average power of the laser was set to 200 mW by using an optical attenuator. The laser pulses were focused into a soda-lime glass substrate (Corning 0215, n=1.515) by using a 1.25-NA 100 times magnification, oil immersion microscope objective lens (Edmund Optics) with immersion oil (n=1.516). The glass substrate was translated by a three-axis air-bearing translating stage (Aerotech), so that the focal point could be scanned freely in the substrate to form three-dimensional waveguide structures. Waveguides were fabricated with a scanning velocity of 8 mm/second. Under these exposure conditions, measurements confirmed that waveguides were single mode at 1500 nm wavelengths [10]. The center-to-center separations between the input and the output waveguides were fixed at 80 μm, while the separation between the waveguides in the coupling region was varied between 15, 20, and 25 μm in order to investigate the coupling characteristics. Ideally, the transition waveguides should be curved in order to connect smoothly to the input and the output waveguides and the coupling waveguides. However, for simplicity of fabrication, we used straight waveguides in this experiment as shown in Fig 1. The horizontal length of the transition waveguide regions was fixed at 5 mm. Therefore, the junction angles between the transition waveguide regions and the input and the output, and the coupling waveguide region, varied from 0.43 to 0.36 degrees, according to the waveguide separation and the length of the coupling region. This variation in angle has a negligible effect on the coupling characteristics.

#10011 - $15.00 USD Received 16 December 2005; revised 3 March 2006; accepted 5 March 2006

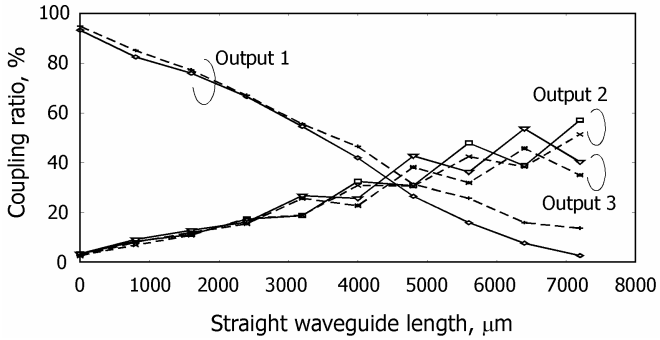

(a)

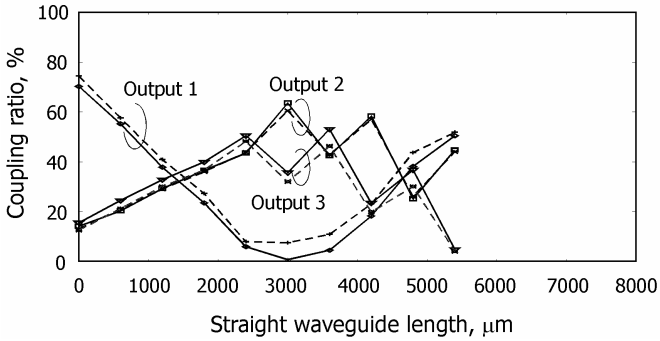

(b)

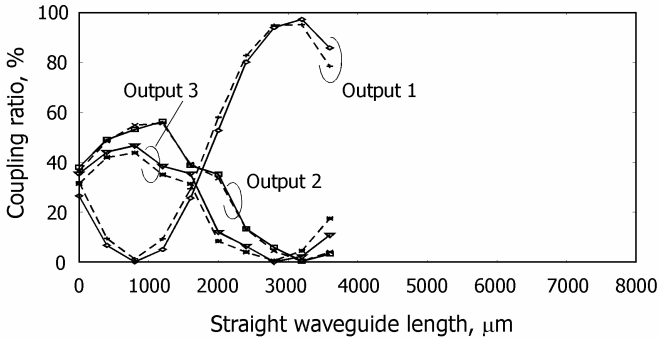

(c)

Fig. 2. Coupling characteristics of a fabricated [3x3] directional coupler with an optical signal from input port 1. The separations between the coupling waveguides S are designed to be (a) 25 μm, (b) 20 μm, and (c) 15 μm. The solid lines and dotted lines correspond to TM and TE polarization modes, respectively.

Figure 2 shows the coupling characteristics of the various [3x3] directional couplers at a wavelength of 1530 nm. The solid and dotted lines represent the coupling characteristics for TM and TE polarized modes, respectively. Only a small polarization dependence of 11 % in the coupling ratio is observed in the coupler with a separation of 25 μm and a coupling interaction length of 7200 μm. This fact supports the idea that a waveguide fabricated with a high-repetition-rate ultra short pulse laser does not show polarization dependence [11]. The measured losses were 6.6 dB and varied only by 0.2 dB as the separation distance was varied from 25 μm to 15 μm. The excess loss includes propagation loss as well as fiber coupling loss. The small loss variation of 0.2 dB with waveguide separation distance means that the losses from the discontinuities between waveguides. This means that the effect of the nonadiabatic connection along transition waveguide is negligible. As shown in Fig. 2, the separation *S* between the waveguides in the coupling region clearly affects the coupling characteristics. For

#10011 - $15.00 USD Received 16 December 2005; revised 3 March 2006; accepted 5 March 2006

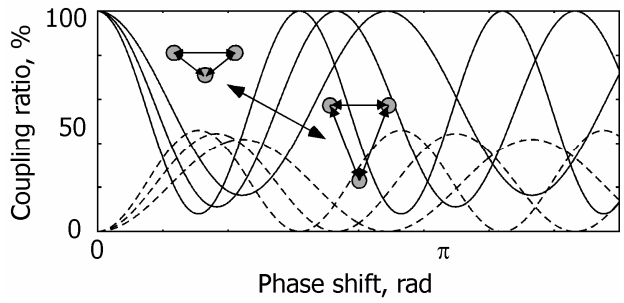

(a)

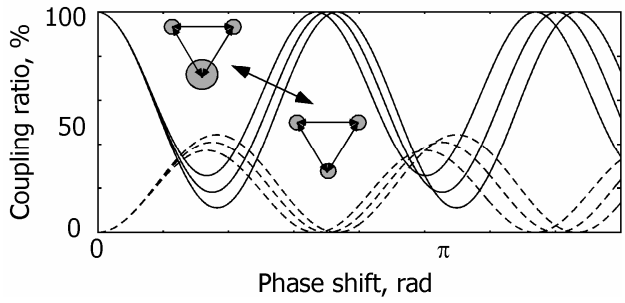

(b)

Fig. 3. Calculated coupling characteristics of [3x3] directional couplers, when (a) the position of waveguide 1 is not aligned correctly, and when (b) the propagation constant of the waveguide is different from the others.

25 μm separation, the measured characteristics are shown on the left-hand side of Fig. 1(b), and starts at almost 0 % coupling for a coupling length of 0 μm. On the other hand, with separations of 20 and 15 μm, a nonzero amount of power has already been transferred when the straight waveguide interaction length is 0 μm. This is because the coupling between the waveguides in the transition region becomes dominant. In either case, the measured coupling characteristics oscillate as a function of the straight waveguide interaction length. This indicates that, despite some errors, it is possible to realize coupled mode functions that are sinusoidal.

However, it should be noted that the optical power of waveguide 1 falls to zero for interaction lengths of the straight waveguide of 7000, 3000, and 800 μm in couplers with waveguide separations of 25, 20, and 15 μm, respectively. This tendency appears systematically for all waveguide separations. In the numerical calculation, it is shown that the optical power of waveguide 1 never falls to zero if the coupler is symmetric. This fact suggests that systematic fabrication errors result in coupler asymmetry.

4. Discussion

Femtosecond laser waveguide fabrication techniques provide a unique approach for fabricating devices such as symmetric [3x3] couplers, which can only be realized using a three-dimensional device design. Measurements of the couplers, as a function of coupling interaction length, have been performed and compared to theoretical predictions. Since each data point represents a different device fabrication, the relatively low scatter in the data shows that fabrication parameters can be relatively well controlled and the device characteristics reproducibly measured.

Coupling effects between the waveguides in the transition region contribute to the observed characteristics because the waveguides entering the interaction region are at small angles of 0.43 to 0.36 degrees. These effects can be accounted for if the design objective is to

#10011 - $15.00 USD Received 16 December 2005; revised 3 March 2006; accepted 5 March 2006

fabricate specific device characteristics. Measurements of transfer characteristics versus coupling interaction length show that there are residual, reproducible fabrication errors in the process. The fabrication errors can be included by adjusting parameters κ_{ij} and/or δ_{ij}. It is natural to anticipate that waveguides 2 and 3 were fabricated identically, because of our fabrication process and the similarity of the measured characteristics of outputs 2 and 3. On the other hand, waveguide 1 is in a different layer from waveguides 2 and 3. This could result in a fabrication error in the vertical position and/or a propagation constant that is different from the other waveguides.

We calculated numerically the effect of asymmetry in waveguide 1 by using the general mode coupling equations of Eq. (1) with the Runge-Kutta method. Figure 3 shows the estimated coupling ratios for asymmetric [3x3] directional couplers. The insets represent arrangements of waveguide 1; that is, in Fig. 3(a), only the vertical position of waveguide 1 is varied, and in Fig. 3(b), the propagation constant of waveguide 1 differs from those of the others. In other words, the calculations assume an asymmetry of $2\kappa_{12} = \kappa_{23} = \kappa_{31}$ and $0.5\kappa_{12} = \kappa_{23} = \kappa_{31}$ in Fig. 3(a) and, $2\delta_{12} = \delta_{23} = \delta_{31}$ and $0.5\delta_{12} = \delta_{23} = \delta_{31}$ in Fig. 3(b). As shown in Fig. 3(a), if waveguide 1 comes closer to the others, the minimum optical power in the waveguide will go to zero for some value of the phase shift or coupling interaction length. In contrast, the minimum power moves away from zero when waveguide 1 is further from the others. Meanwhile, in Fig. 3(b), if we assume that waveguide 1 has a different propagation constant from the others, the minimum optical power also does not go to zero. This tendency is similar to that found in [2x2] couplers [12, 13]. The optical power from output 1 only goes to zero when the waveguide 1 is closer to the others.

Additional supporting evidence for a position error in waveguide 1 is the fact that there is a small refractive index mismatch between the glass substrate and the immersion oil. This mismatch causes a difference between the physical translation of the glass substrate and the focal point of the beam. A simple calculation gives us a relation of

$$\frac{dz_1}{dz_0} = \frac{\tan\theta_0}{\tan\theta_1} \tag{2}$$

$$\theta_0 = \arcsin(\mathrm{NA}/n_0) \tag{3}$$

$$\theta_1 = \arcsin(\mathrm{NA}/n_1) \tag{4}$$

where dz_1, dz_0, n_0 and n_1 are the physical translation of the substrate, the displacement of the focal point, and the refractive indices of the immersion oil and the substrate, respectively. By substituting the values of the experimental configuration, n_0 = 1.516, n_1 = 1.515 and NA = 1.25, we can obtain a ratio of the displacement between the physical translation and the focal point of 99.8 %. Therefore, the vertical translation is smaller than the horizontal translation. This would support the hypothesis that waveguide 1 is closer to the others.

5. Conclusion

In this paper, we fabricated and characterized symmetric three-dimensional [3x3] couplers. The waveguides were fabricated in three dimensions by using a direct waveguide writing technique with a high-repetition-rate femtosecond laser oscillator. The effects of varying interaction length were examined by fabricating couplers with different interaction lengths and by characterizing these devices. The fabricated couplers have characteristics that agree well with theory for a symmetric [3x3] coupler. Coupling in the region of the taper was shown to play an important role in the output characteristics as a function of interaction length. The largest polarization dependence of the coupling ratio was 11% and the maximum insertion loss was 6.7 dB. Even though errors were observed in the fabricated couplers that might cause degradation the coupler performance, comparison to theory shows that these errors are due to an error in the position of one of the waveguides in the vertical direction. These results demonstrate the femtosecond laser fabrication of a representative three-dimensional device, the symmetric [3x3] coupler, the characterization of waveguide characteristics, and a

#10011 - $15.00 USD Received 16 December 2005; revised 3 March 2006; accepted 5 March 2006

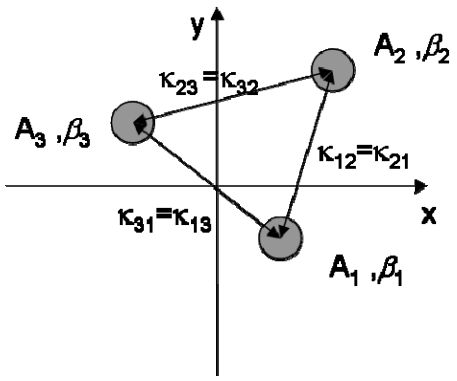

Fig. 4. Cross-sectional diagram of the optical coupling region of a general [3x3] directional coupler.

comparison to theory. Measurements are in good agreement with theory and suggest approaches for improving future performance.

Appendix

General mode coupling equations (1) are derived from Maxwell's equations by following a procedure described in [12] and by expanding it to a situation where three waveguides are arranged closely. Figure 4 shows a cross-sectional diagram of the optical coupling region of a general [3x3] directional coupler.

Maxwell's equations in each waveguide are

$$\begin{aligned} \nabla \times E_p &= -j\omega\mu_0 H_p \\ \nabla \times H_p &= -j\omega\varepsilon_0 N_p^2 E_p \end{aligned} \tag{A-1}$$

where E_p, and H_p are the electric and magnetic fields of the p th waveguide. N_p, ω, ε_0 and μ_0 are the refractive index distribution of the p th waveguide, the angular frequency of the optical signal, the dielectric constant, and the magnetic permittivity in vacuum. Here, p represents the waveguide number, or p = 1, 2, 3. The electromagnetic fields E of the coupled waveguides are

$$\begin{aligned} E &= A_1(z)E_1 + A_2(z)E_2 + A_3(z)E_3 \\ H &= A_1(z)H_1 + A_2(z)H_2 + A_3(z)H_3 \end{aligned} \tag{A-2}$$

These fields must satisfy Maxwell's equations. Therefore,

$$\begin{aligned} \nabla \times E &= -j\omega\mu_0 H \\ \nabla \times H &= -j\omega\varepsilon_0 N^2 E \end{aligned} \tag{A-3}$$

N denotes the refractive index distribution of the entire coupling region. By using the following formula of vector,

$$\begin{aligned} \nabla \times (AE) &= A\nabla xE + \nabla AxE \\ &= A\nabla xE + \frac{dA}{dz}u_z xE \end{aligned} \tag{A-4}$$

we obtain the following equations:

$$(u_z x\overline{E}_1)\frac{dA_1}{dz} + (u_z x\overline{E}_2)\frac{dA_2}{dz} + (u_z x\overline{E}_3)\frac{dA_3}{dz} = 0 \tag{A-5}$$

#10011 - $15.00 USD Received 16 December 2005; revised 3 March 2006; accepted 5 March 2006

$$\left[\left(u_z x\overline{H}_1\right)\frac{dA_1}{dz} - j\omega\varepsilon_0\left(N^2 - N_1^2\right)A_1\overline{E}\right] + \left[\left(u_z x\overline{H}_2\right)\frac{dA_2}{dz} - j\omega\varepsilon_0\left(N^2 - N_2^2\right)A_2\overline{E}\right] + \left[\left(u_z x\overline{H}_3\right)\frac{dA_3}{dz} - j\omega\varepsilon_0\left(N^2 - N_3^2\right)A_3\overline{E}\right] = 0 \tag{A-6}$$

Now, by calculating

$$\begin{aligned}\int_{-\infty}^{\infty}\int_{-\infty}^{\infty}\left[\overline{E}_1^* \cdot (\mathrm{A}-5) - \overline{H}_1^* \cdot (\mathrm{A}-6)\right]dxdy = 0\\ \int_{-\infty}^{\infty}\int_{-\infty}^{\infty}\left[\overline{E}_2^* \cdot (\mathrm{A}-5) - \overline{H}_2^* \cdot (\mathrm{A}-6)\right]dxdy = 0\\ \int_{-\infty}^{\infty}\int_{-\infty}^{\infty}\left[\overline{E}_3^* \cdot (\mathrm{A}-5) - \overline{H}_3^* \cdot (\mathrm{A}-6)\right]dxdy = 0\end{aligned} \tag{A-7}$$

and by separating the transversal and axial dependencies of electromagnetic fields,

$$\begin{aligned}\overline{E}_p &= E_p e^{-j\beta_p z}\\ \overline{H}_p &= H_p e^{-j\beta_p z}\end{aligned} \tag{A-8}$$

we obtain general mode coupling equations for a [3x3] directional coupler.

$$\begin{aligned}&\frac{dA_1}{dz} + c_{12}\frac{dA_2}{dz}e^{-j(\beta_2-\beta_1)} + c_{13}\frac{dA_3}{dz}e^{-j(\beta_3-\beta_1)} + j\chi_1 A_1 + j\kappa_{12}A_2 e^{-j(\beta_2-\beta_1)} + j\kappa_{13}A_3 e^{-j(\beta_3-\beta_1)}\\ &\frac{dA_2}{dz} + c_{23}\frac{dA_3}{dz}e^{-j(\beta_3-\beta_2)} + c_{21}\frac{dA_1}{dz}e^{-j(\beta_1-\beta_2)} + j\chi_2 A_2 + j\kappa_{23}A_3 e^{-j(\beta_3-\beta_2)} + j\kappa_{21}A_1 e^{-j(\beta_1-\beta_2)}\\ &\frac{dA_3}{dz} + c_{31}\frac{dA_1}{dz}e^{-j(\beta_1-\beta_3)} + c_{32}\frac{dA_2}{dz}e^{-j(\beta_2-\beta_3)} + j\chi_3 A_3 + j\kappa_{31}A_1 e^{-j(\beta_1-\beta_3)} + j\kappa_{32}A_2 e^{-j(\beta_2-\beta_3)}\end{aligned} \tag{A-9}$$

Here,

$$\begin{aligned}\kappa_{pq} &= \frac{\omega\varepsilon_0\int_{-\infty}^{\infty}\int_{-\infty}^{\infty}\left(N^2 - N_q^2\right)E_P^* \cdot E_q dxdy}{\int_{-\infty}^{\infty}\int_{-\infty}^{\infty}u_z \cdot \left(E_P^* \times H_p + E_p \times H_P^*\right)dxdy}\\ c_{pq} &= \frac{\int_{-\infty}^{\infty}\int_{-\infty}^{\infty}u_z \cdot \left(E_P^* \times H_q + E_q \times H_P^*\right)dxdy}{\int_{-\infty}^{\infty}\int_{-\infty}^{\infty}u_z \cdot \left(E_P^* \times H_p + E_p \times H_P^*\right)dxdy}\\ \chi_p &= \frac{\omega\varepsilon_0\int_{-\infty}^{\infty}\int_{-\infty}^{\infty}\left(N^2 - N_p^2\right)E_P^* \cdot E_p dxdy}{\int_{-\infty}^{\infty}\int_{-\infty}^{\infty}u_z \cdot \left(E_P^* \times H_p + E_p \times H_P^*\right)dxdy}\end{aligned} \tag{A-10}$$

Here, the second term, the third term, and cpq represent the butt-coupling terms and the butt-coupling coefficient, respectively. The fourth term represents the propagation of the electromagnetic field of the waveguide itself. The last two terms are the mode coupling between waveguides. κ_{pq} is the coupling coefficient between the *p* th and *q* th waveguides. As described in ref [11], when there is sufficient distance between the waveguides, we can ignore the effect of χ_p and c_{pq}. In addition, the relation between reciprocity of the coupling coefficients is

#10011 - $15.00 USD Received 16 December 2005; revised 3 March 2006; accepted 5 March 2006

$$\kappa_{12} = \kappa_{21}^{*}$$
$$\kappa_{23} = \kappa_{32}^{*} \qquad \text{(A-11)}$$
$$\kappa_{31} = \kappa_{13}^{*}$$

In most of the directional couplers, κ_{pq} is real. Finally, we obtain

$$\frac{dA_1}{dz} + j\kappa_{12}A_2 e^{-j2\delta_{21}z} + j\kappa_{13}A_3 e^{+j2\delta_{13}z} = 0$$
$$\frac{dA_2}{dz} + j\kappa_{21}A_1 e^{+j2\delta_{21}z} + j\kappa_{23}A_3 e^{-j2\delta_{23}z} = 0 \qquad \text{(1)}$$
$$\frac{dA_3}{dz} + j\kappa_{31}A_1 e^{-j2\delta_{13}z} + j\kappa_{32}A_2 e^{+j2\delta_{23}z} = 0$$

$$\delta_{21} = \frac{\beta_2 - \beta_1}{2}, \quad \kappa_{12} = \kappa_{21}$$
$$\delta_{32} = \frac{\beta_3 - \beta_2}{2}, \quad \kappa_{23} = \kappa_{32} \qquad \text{(A-12)}$$
$$\delta_{13} = \frac{\beta_1 - \beta_3}{2} \qquad \kappa_{31} = \kappa_{13}$$

Acknowledgments

This research is supported in part by the Air Force Office of Scientific Research Contract F9550-040-1-0011 and the National Science Foundation ECS-0501478. We gratefully acknowledge the contributions of Drs. Andrew Kowalevicz and Kaoru Minoshima in the early phases of this research.